Light-harvesting function of β-carotene inside carbon nanotubes

Kazuhiro Yanagi,[1,*] Konstantin Iakoubovskii,[1] Said Kazaoui,[1] Nobutsugu Minami,[1] Yutaka Maniwa,[2] Yasumitsu Miyata,[1] and Hiromichi Kataura[1]

[1]*Nanotechnology Institute, National Institute of Advanced Industrial Science and Technology (AIST), Tsukuba 305-8562, Japan*

[2]*Department of Physics, Tokyo Metropolitan University, Tokyo 192-0397, Japan*

(Received 31 July 2006; revised manuscript received 31 August 2006; published 18 October 2006)

Single-wall carbon nanotubes (SWCNTs) are attractive components for nanoscale electronics, however their optoelectronic properties have been limited by the optical characteristics of semiconducting SWCNTs. To enhance the functionalities of SWCNTs, β-carotene was encapsulated in SWCNTs and its light-harvesting function was investigated. The detailed structure of encapsulated β-carotene was clarified using x-ray diffraction and the polarization dependence of the optical absorption spectra. The photoluminescence spectra revealed excited energy transfer from β-carotene to the SWCNTs.

DOI: 10.1103/PhysRevB.74.155420 PACS number(s): 78.67.Ch, 78.55.Kz, 78.66.Tr

I. INTRODUCTION

The unique properties of single-wall carbon nanotubes (SWCNTs), such as their high aspect ratio, strength, resonant optical absorption, high carrier mobility, and maximum current densities, make them an attractive component for nanometer scale optoelectronic devices.[1] Recently, the efficient generation[2,3] and detection (quantum efficiency $>10\%$) (Ref. 4) of light by a single SWCNT has been demonstrated. However, the spectral range of these unique devices is limited by the specific density of states of the semiconducting SWCNTs. Controllable modification of the spectral range is required to create efficient optoelectronic devices for SWCNTs.

This modification can be achieved by combining a SWCNT with an appropriate molecule (the so-called "nanotube functionalization"). Such functionalization is commonly achieved by a chemical reaction attaching a molecule outside the SWCNT. Unfortunately, this process has undesirable side effects, such as the creation of defects, as well as quenching the optical absorption and luminescence in SWCNTs. A gentler and more elegant functionalization strategy is to encapsulate organic molecules inside the SWCNT without breaking the chemical bonds.[5,6] It is not yet well known however which molecules are capable of changing the optical properties of SWCNTs via encapsulation.

The encapsulation of β-carotene [a carotenoid (Car) with a chemical structure as shown in Fig. 1(a)] in SWCNTs has been reported in our recent study.[7] We refer to the produced complex as Car@SWCNTs. It is well known that carotenoids exhibit a light-harvesting function in the pigment-protein complexes of photosynthetic bacteria.[8] Thus one might expect similar light-harvesting by β-carotene in Car@SWCNTs complexes as well. We investigated this possibility in this present study.

In pigment-protein complexes, knowledge of the detailed positions of carotene and other pigments allows to control the light-harvesting process.[9] Therefore it is crucial to reveal the structure of the encapsulated dye to understand the energy transfer processes in the dye-SWCNT complexes. In Ref. 7, encapsulation of β-carotene inside SWCNTs has been clarified by optical absorption and Raman measurements.[7] However, detailed structure and functions of encapsulated β-carotene has not been clearly revealed.

Encapsulated β-carotene is not a robust molecule like C_{60}. (The Raman and absorption peaks originating from β-carotene inside the SWCNT disappear upon annealing at approximately 200 °C for 1 h in vacuum.) Therefore, although it is known that high-resolution transmission electron microscopy (HRTEM) measurements can directly probe the encapsulation inside SWCNTs, it is difficult to determine the detailed structure of the encapsulated β-carotene through HRTEM measurements because the electron beam radiation would be strong enough to damage the encapsulated β-carotene. Therefore, in this paper, we studied the structure

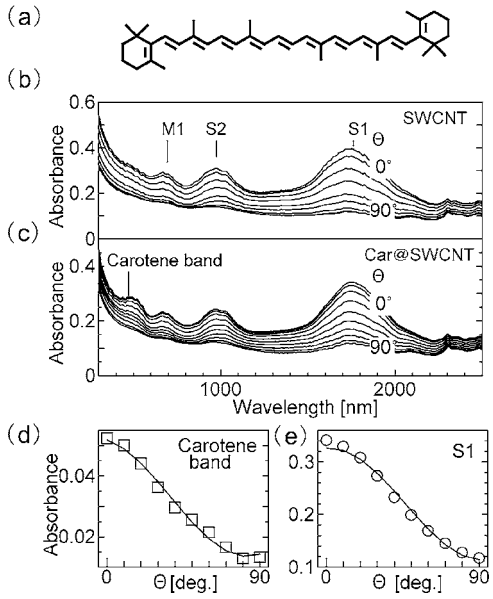

FIG. 1. (a) Chemical structure of β-carotene, and dependence of the absorption spectra of SWCNT (b) and Car@SWCNT (c) on the angle Θ between the stretching direction of the film samples and the polarization of incident linearly polarized light. The absorption feature associated with the encapsulated β-carotene is labeled as the carotene band. Absorption intensities of the carotene (squares) and S1 (circles) bands are plotted as functions of Θ in (d) and (e), respectively, and simulated (solid lines) by $A_i+B_i \cos \Theta^2$ functions.

of encapsulated β-carotene using nondestructive techniques of x-ray diffraction and the polarization dependence of the optical absorption spectra. In addition, photoluminescence (PL) was employed to reveal the energy transfer from β-carotene to the SWCNTs.

II. EXPERIMENTAL SECTION

A. Sample preparation

We used SWCNT manufactured by laser vaporization in an Ar atmosphere of carbon rods doped with Co and Ni. The tubes were purified with H_2O_2, HCl, and NaOH reagents as described previously[10] and then annealed in air at 420 °C for 20 min. The encapsulation of β-carotene into the SWCNTs was performed as follows. SWCNTs (1 mg) and β-carotene (100 mg, Wako) were dissolved in hexane (100 ml). The mixture was refluxed for 10 h in an N_2 atmosphere. Then the solution was filtered and washed with tetrahydrofuran (THF) several times to remove nonencapsulated β-carotene molecules. In order to prepare proper nonencapsulated reference samples, the same procedure has been repeated without β-carotene except for x-ray diffraction (XRD) measurements.

For polarization-resolved absorption measurements, we prepared stretched polymer films where SWCNTs were dispersed and aligned to the stretched direction. The films were prepared as follows. SWCNTs were dispersed in 1% water solution (5 ml) of deoxycholic acid sodium salt (Tokyo Kasei Co.). Polyvinyl alcohol polymer (Kanto Chemical Co., PVA2000) was added to the solution, and then it was dried in a desiccator. The obtained films were mechanically stretched up to 4 times at 70 °C.

PL and unpolarized absorption measurements were performed on solutions (1 cm thick silica cells) prepared with the following procedure. Nanotubes were dispersed for 15 min in 1% D_2O solutions of sodium dodecyl-benzene sulfonate using a tip sonifier (20 kHz, power 100 W). The dispersions were ultracentrifuged for 5 h at 150 000 g, and the upper 80% supernatant was collected.

B. XRD measurement

XRD patterns were recorded using synchrotron radiation with a wavelength of 0.100 nm at the BL1B beam line at the Photon Factory, KEK, Japan. All the XRD measurements were performed at 330 K in vacuum on powder samples.

C. Optical characterization

Optical absorption spectra were recorded with a commercial Shimadzu spectrophotometer. PL mapping was performed with a home-built setup utilizing a tunable Ti-sapphire laser (Spectra-Physics 3900S) or Xe lamp and monochromator for excitation and a single-grating monochromator with an InGaAs diode array for detection.

III. RESULTS AND DISCUSSION

A. Polarization-resolved optical absorption

Our previous Raman measurements on Car@SWCNT indicate the *trans*-conformation of the encapsulated β-carotene.[7] Note that β-carotene is a one-dimensional π-conjugated molecule, thus it is expected to align to the SWCNT axis after encapsulation. Therefore, the optical absorption originating from the encapsulated β-carotene (carotene band) should exhibit the same polarization dependence as the host SWCNT. Figures 1(b) and 1(c) present variations in the absorption spectra of the stretched polymer films of Car@SWCNT and SWCNT with the angle Θ between the stretching direction and the polarization vector of the incident linearly polarized light. Figure 1 reveals that the carotene band exhibits dependence on the polarization angle very similar to that of the absorption bands of the SWCNTs. These bands are labeled Si and Mi, $i=1-2$, and they originate from the ith interband excitations in semiconducting and metallic SWCNTs, respectively. The absorption intensities of the carotene band (squares) and the Si band (circles) are plotted vs Θ in Figs. 1(d) and 1(e), respectively. Both intensities fit very well with the $A_i+B_i\cos\Theta^2$ functions (lines), where constants A_i account for the incomplete SWCNT alignment. The determined absorbance polarization $\rho=(\alpha_{\parallel}-\alpha_{\perp})/(\alpha_{\parallel}+\alpha_{\perp})$ values of the carotene band ($\rho=0.6$) are almost the same as that of the S1 band ($\rho=0.5$). These results clearly indicate that the encapsulated β-carotene molecules are aligned to the SWCNT axis.

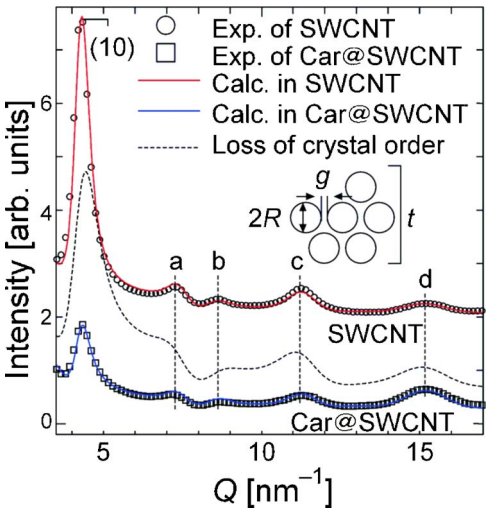

FIG. 2. (Color online) X-ray diffraction patterns of SWCNT (upper curve) and Car@SWCNT (bottom curve). Circles are experimental observations, and the solid red (blue) line is the simulation result for SWCNT (Car@SWCNT). R, g, and t are the radius of SWCNT, intertube distance, and thickness of the nanotube bundle, respectively. Dashed black line shows the calculated XRD pattern assuming the loss of crystal order.

B. XRD results and their modeling

Figure 2 summarizes XRD results. The circles (top curve) present diffraction pattern from the initial SWCNT powder, which has not been subjected to the encapsulation or associated refluxing and/or washing treatment. The profile is dominated by the (10) peak around $Q\equiv 4\pi\sin\theta/r=4.5$ nm^{-1} originating from XRD on SWCNT bundles. The squares (bottom curve) in Fig. 2 show the profile from

Car@SWCNT. It reveals that the encapsulation procedure results in strong quenching of the (10) peak. There are two possible reasons for this decrease: loss of crystal order in the SWCNT bundles or presence of molecules inside the SWCNTs.[11] In order to distinguish between those two possibilities and to obtain the detailed structural information, we performed a numerical simulation of these XRD patterns with reference to Refs. 12 and 13. In this simulation, both the encapsulated molecules and the SWCNT walls were approximated by infinitely thin sheets of homogeneous electron density within the carbon covalent networks.

First, we analyzed the XRD pattern of empty SWCNTs: The SWNTs of the radius R are separated by the distance g and compose a bundle of thickness t (see inset in Fig. 2); the radius R is allowed to spread by the value ΔR. This model was successfully fitted into the profile of the nonencapsulated SWCNTs (see solid red line in Fig. 2), yielding the values of $R=0.69\pm0.01$ nm, $\Delta R=0.06$ nm, $g=0.32\pm0.01$ nm, and $t=17$ nm in agreement with previous results.[12,13] The determined values of R, ΔR, and g were assumed to be unaffected by the encapsulation procedure applied here and thus fixed in the further simulations.

The loss of crystal order upon the encapsulation procedure, as a possible reason for the quenching of the (10) peak, was modeled by decreasing the bundle size t. Dashed black line in Fig. 2 presents simulation obtained with $t=7$ nm. Clearly, it accounts for the reduction in the (10) peak, but also results in the concomitant broadening of all peaks. This broadening is inconsistent with the experiment suggesting that the loss of crystal order hardly occurred during the encapsulation procedure. It is noteworthy that disorder would enhance the D-band and no enhancement was observed in the Raman results for Car@SWCNT.[7] Therefore, the determined above optimal bundle size $t=17$ nm was also fixed in further simulations of Car@SWCNT.

Encapsulation of molecules was modeled by putting them inside the SWCNTs and separating them from the SWCNT walls by the distance δ [see Fig. 3(a)]. We observed a strong dependence of the simulated XRD pattern on the distance δ, as demonstrated in Fig. 3(b). As expected, the encapsulation of molecules in SWCNTs also causes the decrease of (10) peak. Another adjustable parameter in this model is the weight percent w of encapsulated molecules inside SWCNT. In Fig. 3, w is set to be 13%. This parameter changes the (10) peak intensity, but it has minor effect on other profile features. The remarkable feature of the XRD pattern in Car@SWCNT is that the intensity of peak d is larger than that of peak c. It is clear that this remarkable feature can only be reproduced at around the distance $\delta=0.4$. The loss of crystal order cannot reproduce this feature. The best fit could be obtained with $\delta=0.4$ nm and $w=12\%$ (see blue solid line in Fig. 2).

The effect of intercalation on the XRD pattern was reported in Ref. 14. The intensity of the (10) peak decreases with increasing intercalation levels. However, the line shape and position of the (10) peak are broadened and shifted to lower Q, respectively. Thus the effect of intercalation cannot account for the XRD pattern of Car@SWCNT.

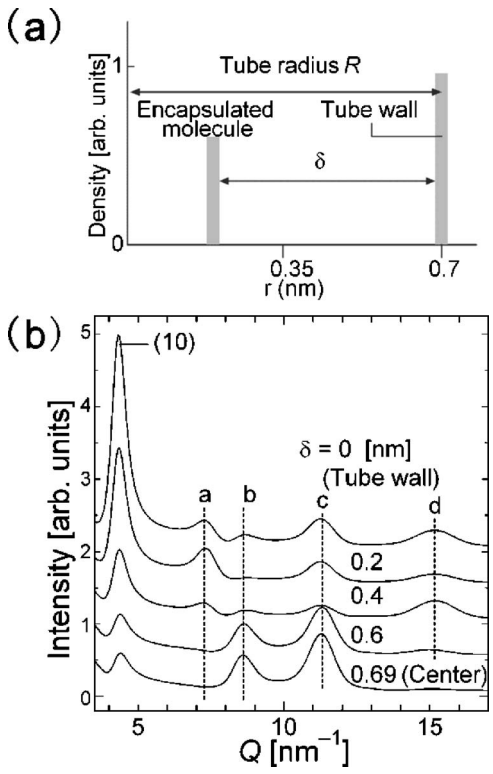

FIG. 3. (a) Simulation model for XRD pattern of Car@SWCNT. (b) The XRD patterns calculated when the distance δ from the encapsulated molecule to the nanotube wall is changed from 0 to 0.69 nm (center of the tube).

C. Analysis of the XRD results

The results of the preceding section suggest the presence of encapsulated molecules, with the weight percent of ~12%, inside the nanotubes of the Car@SWCNT sample. The weight percent of β-carotene alone has been independently estimated as ~3% from optical absorption measurements.[7] (If we assume that β-carotene is present in a line inside a 1.4 nm diameter SWCNT, the filling rate is estimated to be approximately 30%, thus β-carotene is efficiently encapsulated.) There is a difference in the estimated weight percent between encapsulated molecules and encapsulated β-carotene. The difference indicates that the comparable amounts of solvent molecules and β-carotene were encapsulated into the Car@SWCNT nanotubes.

Therefore the derived distance δ between the encapsulated molecules and the tube wall does not directly reflect the position of β-carotene. However, considering the strong sensitivity of the XRD profile to the position of the molecule inside the SWCNT [see Fig. 3(b)], the derived distance δ suggests that both the solvent molecules and β-carotene are positioned off the SWCNT center at a distance of ~0.4 nm to its walls.

The off center location of the encapsulated molecules is remarkable and suggests an attractive interaction with the SWCNT walls. Note that the derived distance between the encapsulated molecules and the SWCNT walls (0.4 nm) is similar to that predicted theoretically (0.33 nm) for the polyacetylene@SWCNT system.[15] It is also similar to the

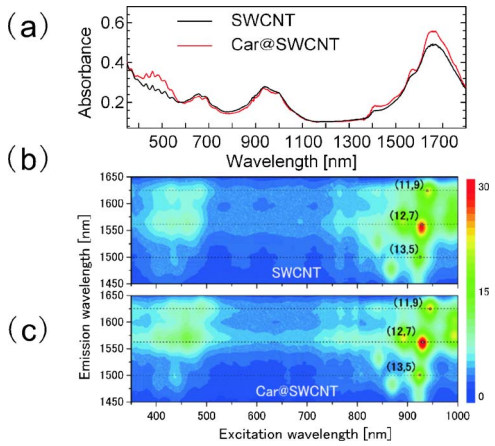

FIG. 4. (Color online) (a) Absorption spectra of the samples used in photoluminescence (PL) measurements. Also shown are PL maps of SWCNT (b) and Car@SWCNT (c) dispersions. Dotted lines indicate excitation profiles for the major SWCNT chiralities, identified as (11,9), (12,7), and (13,5).

distance between the two-dimensional graphitic layers.[16] Therefore, it could be π-π interaction which shifts the encapsulated molecules off center of the SWCNTs.

D. Photoluminescence excitation spectra

Figures 4(b) and 4(c) present 2D maps of the PL excitation and/or emission peak intensities in the SWCNT and Car@SWCNT, respectively. Figure 4(a) shows the corresponding absorption spectra measured from the same solutions. Here the density of the sample solution of Car@SWCNT, which was estimated from the peak intensity of S2 band (940 nm), was adjusted to be the same as that of SWCNT. No luminescence could be detected in the emission range of the isolated β-carotene. Although the luminescence of the β-carotene was completely quenched by encapsulation, PL signals originating from the nanotubes were easily detected and assigned to the (11,9), (12,7), and (13,5) tubes.[17] Note that the radii of the (11,9), (12,7), and (13,5) tubes (0.69, 0.66, and 0.64 nm, respectively) are similar to those estimated from the XRD results (0.69 nm).

The peaks in the PL excitation (PLE) range 800 nm to 1000 nm in Fig. 4 originate from excitation into the S2 band followed by emission from the S1 band. Two processes could account for the features in the excitation range of 350 nm to 600 nm for the Car@SWCNT sample: (i) direct excitation into the S3 band of SWCNT, and (ii) absorption by β-carotene followed by energy transfer to the SWCNT bands. To reveal the latter contribution, we evaluated the difference excitation spectra ΔPLE between the SWCNT and Car@SWCNT for the (11,9), (12,7), and (13,5) tubes [see Figs. 5(b)–5(d), respectively]. The ΔPLE signals were derived as follows: PLE spectra of the S1 emission were extracted for each tube as indicated by the dotted lines in Figs. 4(b) and 4(c). Those spectra were normalized by intensity in the 600 nm to 800 nm region where the contribution of β-carotene is negligible. The normalization was necessary to compensate for slight differences in the dispersion condition

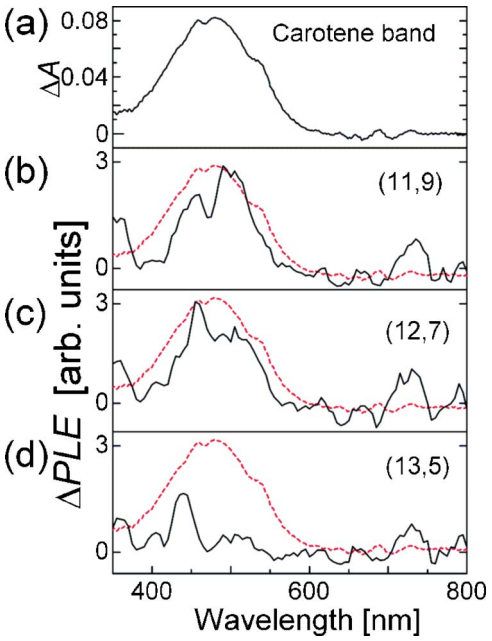

FIG. 5. (Color online) (a) presents the difference absorption spectrum ΔA between Car@SWCNT and SWCNT revealing the carotene band. (b), (c), and (d) show the difference excitation spectra ΔPLE between Car@SWCNT and SWCNT for the (11,9), (12,7), and (13,5) tubes, respectively. The carotene band is also shown with the dashed red line for comparison.

in the SWCNT and Car@SWCNT samples. Then the SWCNT spectra were subtracted from the Car@SWCNT curves thus revealing the β-carotene contribution to the PLE spectra in Car@SWCNT.

Figure 5(a) shows the absorption of the carotene band obtained as the difference between the absorption of Car@SWCNT and SWCNT [Fig. 4(a)]. Remarkably, the difference PLE spectra, which are similar to the carotene absorption band (dotted red lines), were clearly observed for

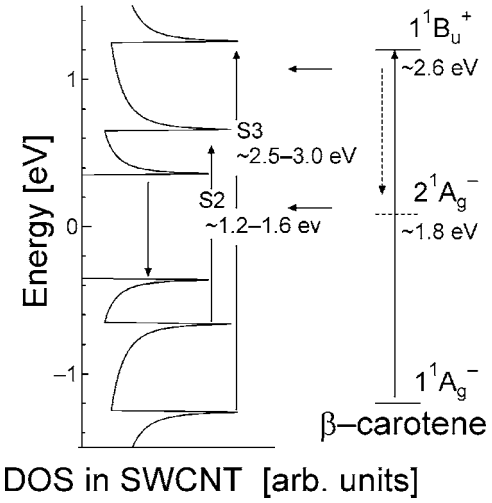

FIG. 6. Schematic illustration of energy transfer processes from β-carotene to SWCNT which might occur after photoexcitation of the $1\,{}^1B_u^+$ excited state of β-carotene.

the (11,9) and (12,7) [Figs. 5(b) and 5(c)], but not for the (13,5) tubes [Fig. 5(d)]. This observation suggests that photoexcitation can be transferred from β-carotene to the SWCNTs, but only to those with relatively large diameters. It can be interpreted that the SWCNTs with small diameters could not incorporate β-carotene.

E. Energy transfer from β-carotene to SWCNT

It is commonly known that there are two important singlet excited states in β-carotene for excited energy transfer, $1\,^1B_u^+$ and $2\,^1A_g^-$.[8,18] Optical transition between the $1\,^1B_u^+$ and the ground $1\,^1A_g^-$ state are allowed (transition energy $E \sim 2.6$ eV), but between the $2\,^1A_g^-$ and $1\,^1A_g^-$ states ($E \sim 1.8$ eV) are symmetry forbidden.[18] When β-carotene is encapsulated in SWCNT the energy of $1\,^1A_g^-$-$1\,^1B_u^+$ transition decreases by $\sim$0.1 eV, as revealed by optical absorption.[7] Comparison of those energies with the SWCNT transitions reveals that the energies of the two excited states of β-carotene overlap with the S3 (2.5–3.0 eV) and S2 (1.2–1.6 eV) transitions. Figure 6 shows a schematic illustration of the possible energy transfer processes from β-carotene to SWCNT. These revealed near-resonant excitation conditions might be responsible for the experimentally observed energy transfer from β-carotene to SWCNT.

IV. CONCLUSION

β-carotene can be efficiently encapsulated in SWCNT, and the detailed structure and optical properties of the encapsulated β-carotene are clarified. The polarization dependence of absorption spectra indicates that encapsulated β-carotene is aligned to the tube axis. This experimental observation suggests that the encapsulation of molecules inside SWCNT can be used to orient molecules. Analysis of the XRD pattern of Car@SWCNT suggests that the encapsulated β-carotene, as well as the solvent, molecules are shifted off the nanotube center. PL measurements indicate that encapsulated β-carotene can transfer photoexcitation energy to the SWCNT, and thus does exhibit the light-harvesting function. We hope that this new and exciting observation will open the door for the fine-tuning, via the encapsulation of various molecules, of the optical properties of SWCNTs for numerous optoelectronic applications.

ACKNOWLEDGMENTS

One of the authors (K.Y.) acknowledges Grant-in-Aid from the Foundation of Advanced Technology Institute, the Sumitomo Foundation (Grant No. 050645), and JSPS.KAKENHI(18740187). This study was supported in part by the Industrial Technology Research Grant Program in 2003 from the New Energy and Industrial Technology Development Organization (NEDO) of Japan.

*Corresponding author. Electronic address: k-yanagi@aist.go.jp

[1] T. Dürkop, B. M. Kim, and M. S. Fuhrer, J. Phys.: Condens. Matter **18**, R553 (2004).
[2] J. A. Misewich, R. Martel, P. Avouris, J. C. Tsang, S. Heinze, and J. Tersoff, Science **300**, 783 (2003).
[3] J. Chen, V. Perebeinos, M. Freitag, J. Tsang, Q. Fu, J. Liu, and P. Avouris, Science **310**, 1171 (2005).
[4] M. Freitag, Y. Martin, J. A. Misewich, R. Martel, and P. Avouris, Nano Lett. **3**, 1067 (2003).
[5] B. W. Smith, M. Monthioux, and D. E. Luzzi, Nature (London) **396**, 323 (1998).
[6] T. Takenobu, T. Takano, M. Shiraishi, Y. Murakami, M. Ata, H. Kataura, Y. Achiba, and Y. Iwasa, Nat. Mater. **2**, 683 (2003).
[7] K. Yanagi, Y. Miyata, and H. Kataura, Adv. Mater. (Weinheim, Ger.) **18**, 437 (2006).
[8] N. J. Fraser, H. Hashimoto, and R. J. Cogdell, Photosynth. Res. **70**, 249 (2001).
[9] R. Z. Desamero, V. Chynwat, I. v. d. Hoef, F. J. Jansen, J. Lugtenburg, D. Gosztola, M. R. Wasielewski, A. Cua, D. F. Bocian, and H. A. Frank, J. Phys. Chem. B **102**, 8151 (1998).
[10] H. Kataura, Y. Maniwa, T. Kodama, K. Kikuchi, K. Hirahara, K. Suenaga, S. Iijima, S. Suzuki, Y. Achiba, and W. Krätschmer, Synth. Met. **121**, 1195 (2001).
[11] Y. Maniwa, Y. Kumazawa, Y. Saito, H. Tou, H. Kataura, H. Ishii, S. Suzuki, Y. Achiba, A. Fujiwara, and H. Suematsu, Jpn. J. Appl. Phys., Part 2 **38**, L668 (1999).
[12] M. Abe, H. Kataura, H. Kira, T. Kodama, S. Suzuki, Y. Achiba, K. I. Kato, M. Takata, A. Fujiwara, K. Matsuda, and Y. Maniwa, Phys. Rev. B **68**, 041405(R) (2003).
[13] H. Kadowaki, A. Nishiyama, K. Matsuda, Y. Maniwa, S. Suzuki, Y. Achiba, and H. Kataura, J. Phys. Soc. Jpn. **74**, 2990 (2005).
[14] X. Liu, T. Pichler, M. Knupfer, and J. Fink, Phys. Rev. B **67**, 125403 (2003).
[15] G. C. McIntosh, D. Tománek, and Y. W. Park, Phys. Rev. B **67**, 125419 (2003).
[16] S. Bandow, F. Kokai, K. Takahashi, M. Yudasaka, L. C. Qin, and S. Iijima, Chem. Phys. Lett. **321**, 514 (2000).
[17] R. B. Weisman and S. M. Bachilo, Nano Lett. **3**, 1235 (2003).
[18] K. Onaka, R. Fujii, H. Nagae, M. Kuki, Y. Koyama, and Y. Watanabe, Chem. Phys. Lett. **315**, 75 (1999).